



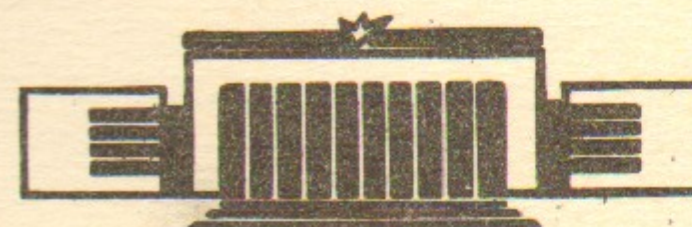
ИНСТИТУТ ЯДЕРНОЙ ФИЗИКИ СО АН СССР

55

**G.V. Anikin, L.M. Barkov, B.I. Hasin, V.S. Okhapkin,**  
S.I. Redin, N.M. Riskulov, Yu.M. Shatunov,  
A.I. Shekhtman, A.N. Skrinsky,  
V.P. Smakhtin, E.P. Solodov

THE RESULTS OF EXPERIMENTS WITH  
CMD ON VEPP-2M STORAGE RING

PREPRINT 83—85



НОВОСИБИРСК

## 1. Introduction

To study the  $e^+e^-$  annihilation on VEPP-2M storage ring [1] the Cryogenic Magnetic Detector (CMD) has been used. The sketch of the CMD is drawn on Fig. 1. The six-gaps cylindrical optical spark chamber (6) is inserted inside superconductive solenoid (7) with the maximum working magnetic field 32 kGs. The solenoid and spark chamber axes are parallel to the beam motion direction. The spark chamber operates at the temperature about 170-180 K and pressure about 2 atm. The high gas density (3.5 times greater than at normal condition) allows to obtain spatial resolution  $\sim 50 \mu\text{m}$ . Two cylindrical MPC were used to trigger the spark chamber. The gas mixture of the spark chamber and the MPC's are the same.

The solid angle of the detector is equal to  $0.6 \times 4\pi$  str. Only charged particles are detected. The momentum resolution of the CMD is  $\Delta p/p = 2.5\%$  for  $p = 500 \text{ MeV}/c$ . [2].

In this paper the results of following experiments are presented:

The charged pion formfactor in the energy region  $0.36 \text{ GeV} \leq 2E \leq 0.820 \text{ GeV}$  has been measured. These measurements with the results of other experiments permit to obtain the electromagnetic radius of the pion, the  $\rho^0$ -meson parameters and the hadronic vacuum polarization contribution in the anomalous magnetic moment of the muon, which strongly depends on the hadrons production cross-section in the quoted energy region.

The electromagnetic formfactors of charged and neutral kaons and cross-sections of four and five pions production are presented at four energy points  $2E = 1.088, 1.202, 1.270$  and  $1.348 \text{ GeV}$ .

The precise measurement of the neutral kaon mass with the resonance depolarization calibration of the beam energy is also presented.

## 2. The $e^+e^- \rightarrow \pi^+\pi^-$ reaction

The squared formfactor of the charged pion has been measured at 19 fixed values of the colliding beams energy. Among the events obtained in each energy point the collinear events, satisfying the following criteria were selected:

- the angle between tracks in the plain transversal to the beam axis  $|\Delta\varphi| < 6^\circ$ ,
- the angle between tracks in the plain containing the beam axis  $|\Delta\theta| < 10^\circ$ ,
- the average distance between tracks and beam axis  $\Delta r < 0.15$  cm,
- the particles momentum differs less than 15%.

The identification of the selected events with the events of the  $e^+e^-$ ,  $\mu^+\mu^-$  and  $\pi^+\pi^-$  pair production have been made with the help of the likelihood function method. As an example, the distributions of the collinear events as a function of the average momentum for three energy points are shown in Fig. 2. The full lines are the theoretical curves evaluated with the maximum likelihood function method.

In the Table 1 for each energy point the integrated luminosity (L); the numbers of electron's (Ne), muons ( $N_\mu$ ), pions ( $N_\pi$ ), background events ( $N_B$ ), obtained as a result of separation, the ratio  $N_\pi / (N_e + N_\mu)$  and the square of pion formfactor are listed.

The squared pion electromagnetic formfactor was calculated by the expression:

$$|F_\pi|^2 = \frac{N_\pi}{N_e + N_\mu} \cdot \frac{\sigma_e(1-\delta_e) + \sigma_\mu(1-\delta_\mu)}{\sigma_\pi(1-\delta_\pi)(1-\delta_\pi^N)(1-\delta_\pi^D)},$$

where  $\sigma_e, \sigma_\mu, \sigma_\pi$  - are the detection cross-sections for the reactions  $e^+e^- \rightarrow e^+e^-$ ,  $\mu^+\mu^-$ ,  $\pi^+\pi^-$ , correspondingly, calculated in the first Born approximation of QED,  $\delta_e, \delta_\mu, \delta_\pi$  - the radiative corrections for mentioned cross-sections calculated with the accuracy of the order  $\alpha^3$  in accordance with [3].

$\delta_\pi^N, \delta_\pi^D$  - the corrections on nuclear capture of pions in the

Table 1

2E	$L, \text{nb}^{-1}$	Ne	$N_\mu$	$N_\pi$	$N_B$	$N_\pi / (N_e + N_\mu)$	$ F_\pi ^2$
0.360	5.7	10070	936	164	360	0.015±0.001	1.87±0.16
0.380	4.1	5853	477	135	227	0.021±0.002	2.13±0.20
0.410	3.2	6033	515	190	225	0.029±0.002	2.37±0.16
0.430	1.7	3172	239	114	96	0.034±0.003	2.44±0.24
0.438	3.4	3603	353	159	84	0.040±0.003	2.77±0.23
0.470	4.2	5000	488	250	102	0.044±0.003	2.77±0.18
0.540	2.4	3029	311	294	36	0.088±0.008	4.45±0.30
0.580	1.9	2020	197	260	14	0.117±0.008	5.63±0.38
0.620	2.2	2026	191	429	32	0.133±0.011	8.62±0.50
0.640	2.3	2035	182	509	77	0.222±0.012	9.87±0.55
0.660	0.9	784	68	266	23	0.312±0.024	12.60±0.89
0.700	0.3	260	23	170	23	0.592±0.064	25.37±2.74
0.740	0.4	253	23	308	22	1.110±0.101	45.45±4.09
0.760	0.7	473	43	583	54	1.039±0.071	40.90±2.79
0.780	0.7	419	38	537	31	1.176±0.086	45.01±3.29
0.790	1.6	986	89	879	84	0.818±0.045	30.54±1.68
0.794	1.5	921	83	775	93	0.772±0.044	28.82±1.64
0.800	0.6	379	34	304	39	0.735±0.068	27.04±2.50
0.820	1.2	659	59	396	50	0.551±0.043	19.39±1.51

detector material and on the pions decays in the fiducial volume of the spark chamber.

The systematical error in  $|F_\pi|^2$  is connected with the inaccuracy in radiative corrections evaluation (1%), uncertainty in nuclear absorption (1%) and decay corrections (1%) and doesn't exceeds 2% in each energy point.

The experimental data on  $|F_\pi|^2$  dependence on  $2E = \sqrt{S}$  in the region  $S > 4m_\pi^2$  taken from works [4-13] and this experiment are shown in Fig. 3. To fit all the data the models including resonances  $\rho, \omega$  and  $\rho'(1600)$  or  $\rho'(1250)$  were tried. The dependence of  $\rho$ -meson width versus energy was treated on the ground of Gounaris-Sakurai model [14] as well,

as on the model, described in the [15]. To evaluate the models parameters the systematical errors of the experimental data have been taken into account as well, as the statistical errors. The solid line in Fig. 3 represents one of the fits that differs very little from others. As a result of fits the following parameters of  $\rho^0$ -meson have been found:

$$M_\rho = 775.8 \pm 1.6 \text{ MeV}$$

$$\Gamma_\rho = 146.9 \pm 2.6 \text{ MeV.}$$

The model dependence of  $\rho^0$ -meson parameters is substantially less than statistical and systematical errors. The mean square electromagnetic radius of pion was determined by differentiation of extrapolated to  $S = 0$  model curves:

$$\langle r_\pi \rangle^2 = (0.414 \pm 0.002 \pm 0.003(\text{model})) \text{ fm}^2.$$

The first error corresponds to statistical and systematical uncertainties in  $|F_\pi|^2$ . The second error was estimated as a maximal deviation of  $\langle r_\pi \rangle^2$  value for different models.

The information about  $e^+e^-$  annihilation into the pairs of charged pions, obtained in this experiment, allows to improve substantially the precision of hadronic vacuum polarization contribution  $a_H$  in the anomalous magnetic moment of the muon  $a_\mu$  [16, 17].

The fit of the experimental data in the region  $4m_\pi^2 \leq S \leq 1 \text{ GeV}^2$ , gives for the value  $a_H^{\pi^+\pi^-}$

$$a_H^{\pi^+\pi^-} = (47.46 \pm 0.57) \cdot 10^{-9}.$$

The contribution in  $a_H$  from other hadron channels and the energy region above 1 GeV determined from presently known experimental data on  $R = \sigma(e^+e^- \rightarrow \text{hadrons}) / \sigma(e^+e^- \rightarrow \mu^+\mu^-)$  is equal to

$$a_H^{\text{hadrons}} = (17.80 \pm 0.93) \cdot 10^{-9},$$

thus the total value of hadronic vacuum polarization is

$$a_H = (65.26 \pm 1.1) \cdot 10^{-9}.$$

Taking into account the computed in [18] electromagnetic cont-

tribution

$$a_{\text{QED}} = (1165852 \pm 1.9) \cdot 10^{-9}$$

and weak contribution

$$a_W = (2.1 \pm 0.2) \cdot 10^{-9}$$

the anomalous magnetic moment of the muon is expected to be:

$$a_{\mu\text{theor.}} = a_{\text{QED}} + a_H + a_W = (1165919, 1 \pm 2.2) \cdot 10^{-9},$$

that should be compared with the last most precise experimental value [17]

$$a_{\mu\text{exp}} = (1165924 \pm 8.5) \cdot 10^{-9}.$$

### 3. The $e^+e^- \rightarrow K^+K^-$ reaction

To separate the events of charged kaon pairs production were imposed demands analogous to those described in the previous chapter.

The separation of the events were performed by means of average momentum of two particles. The distributions of selected events on average momentum at four energy points are shown in Fig. 5. One can see, that there are no difficulties in separation of two charged kaons events from pairs of electrons, muons and pions in quoted energy region. The subtraction of cosmic particles background was made with the assumption that the momentum distribution of background events in the region of interest is uniform, that can be seen in Fig. 5.

The results of events identification are listed in Table 2. The table contains the total number of collinear events ( $N_{\text{tot}}$ ), the number of events in the kaon peak ( $N_K$ ), the number of events in the electrons, muons and pions bump ( $N_e$ ), the number of events between peaks ( $N_B$ ), the calculated numbers of events in the peaks of kaons and electrons ( $N_{Bk}$ ,  $N_{ek}$ ) and the numbers of events with production of kaons and  $ee$ ,  $\mu\mu$ ,  $\pi\pi$

pairs after background subtraction ( $N_K - N_{BK}$ ;  $N_e - N_{Be}$ ).

Table 2

$2E, \text{GeV}$	$N_{\text{tot}}$	$N_K$	$N_e$	$N_B$	$N_{BK}$	$N_{Be}$	$N_K - N_{BK}$	$N_e - N_{Be}$
1.088	1683	39	1614	30	4.7	13.7	$34.3 \pm 6.2$	$1600.3 \pm 40.2$
1.202	5656	93	5477	86	12.3	45.0	$80.7 \pm 9.6$	$5432.0 \pm 74.0$
1.270	4859	80	4703	76	12.3	34.3	$67.7 \pm 8.9$	$4668.7 \pm 68.6$
1.348	4786	100	4613	73	15.6	39.0	$84.4 \pm 9.9$	$4574.0 \pm 67.9$

The squared formfactor of the charged kaons was calculated by the expression:

$$|F_{K^\pm}|^2 = \frac{N_K - N_{BK}}{N_e - N_{Be}} \cdot \frac{\sigma_e(1-\delta_e) + \sigma_\mu(1-\delta_\mu) + \sigma_\pi |F_\pi|^2 (1-\delta_\pi)(1-\delta_\pi^N)}{\sigma_K(1-\delta_K)(1-\delta_K^N)(1-\delta_K^D)}$$

where  $\sigma_K, \sigma_e, \sigma_\mu, \sigma_\pi$  are the detection cross-sections for the reactions  $e^+e^- \rightarrow K^+K^-, e^+e^-, \mu^+\mu^-, \pi^+\pi^-$  calculated in the first Born approximation of QED.

$\delta_K, \delta_e, \delta_\mu, \delta_\pi$  - radiative corrections for mentioned reactions calculated in accordance with [3].

$\delta_K^N, \delta_\pi^N$  - corrections for nuclear absorption of kaons and pions in the matter of the chamber evaluated on the ground of the experimental data of [23] and found to be about 4%.

$\delta_K^D$  - the correction on kaon decays in flight that change with energy from 12% to 6%.

$|F_\pi|^2$  - the squared formfactor of the pion, taken from the [13].

The  $e^+e^-, \mu^+\mu^-, \pi^+\pi^-$  events have been used to determine the integrated luminosity in each energy point. The integrated luminosity, cross-section and squared formfactor of charged kaon are listed in Table 3.

The systematical error in  $|F_{K^\pm}|^2$  is about 3% from uncertainty in solid angle of the detector 1%, the error in radiative corrections calculations 1%, uncertainties in nuclear absorption and in decay in flight 2%.

The values of  $|F_{K^\pm}|^2$  from this work together with other data

Table 3

$2E, \text{GeV}$	$L, \text{nb}^{-1}$	$\sigma, \text{nb}$	$ F_{K^\pm} ^2$	$ F_{K^\pm} ^2$ including [24]
1.088	5.0	$12.93 \pm 2.11$	$10.14 \pm 1.86$	$9.73 \pm 1.59$
1.202	22.9	$7.47 \pm 0.89$	$2.68 \pm 0.32$	
1.270	21.5	$6.60 \pm 0.87$	$1.97 \pm 0.26$	
1.348	24.0	$7.24 \pm 0.79$	$1.90 \pm 0.23$	$1.92 \pm 0.21$

in this energy region are presented in the Fig. 6. The values of squared formfactor in the points 1.088 and 1.348 are averaged with our previous work [24]. The solid line represents the VDM with  $\rho, \omega$  and  $\phi$  mesons. Our results are in a good agreement with results of [27].

#### 4. The $e^+e^- \rightarrow K^S K^L$ reaction

The pairs of neutral kaons were detected by decays of short lived kaon in flight on pair of charged pions, which are two prong fork-like events. To separate such decays, the events with the angle of noncollinearity more than  $6^\circ$  were selected. In addition, the following selection criteria were imposed:

- the total energy of both particles (both of them are assumed to be pions) should be within two standard deviations of the detector resolution from the beam energy;
- the point decay should be in the vacuum chamber;
- the missing momentum, of the event differs from calculated kaon momentum at given energy not more than 20%;
- the missing mass with the accuracy of the detector resolution should be equal to the mass of neutral long lived kaon.

For selected events the squared effective mass of two pions were calculated. The summarized distribution of events for all energy points versus that parameter is given in Fig. 7a. The solid line under the squared mass axis indicates the doubled resolution of the detector on that parameter. The events from indicated interval were assumed to be candidates for neutral kaons ( $N_K$ ). The number of background events ( $N_B$ )

in indicated interval was estimated by the number of events out of the interval. For comparison the distribution of the events that didn't satisfied the selection criteria is shown in Fig. 7B. The results of events identification procedure are listed in Table 4. Because of low statistic the two last points are combined.

Table 4

2E, GeV	L, nb <sup>-1</sup>	N <sub>K</sub>	NB	ε, %	σ <sub>K<sup>0</sup></sub> , nb	F <sub>K<sup>0</sup></sub>   <sup>2</sup>
1.088	4.7	3	0	16	4.2+2.6 -2.1	3.4+2.1 -1.7
1.202	21.3	4	0.2	8	2.3+1.4 -1.1	0.87+0.53 -0.42
1.270-1.348	42.4	3	2.8	4	0.12+1.0 -0.12	0.04+0.32 -0.04

The efficiencies have been computed by the Monte-Carlo method. The results of efficiencies calculation (ε), cross-sections of the neutral kaons pair production (σ<sub>K<sup>0</sup></sub>) and squared formfactor (|F<sub>K<sup>0</sup></sub>|<sup>2</sup>) are listed in Table 4 together with integrated luminosity (L). The radiative corrections are about 5%. For cross-sections and squared formfactors at energies 1.270-1.348 GeV the upper limits could be estimated σ<sub>K<sup>0</sup></sub> < 1.6 nb, |F<sub>K<sup>0</sup></sub>|<sup>2</sup> < 0.48 (90% C.L.).

The systematical error is connected mainly with efficiencies computation and is equal approximately to 10%.

The experimental data on neutral kaon squared formfactor above 1.1 GeV are shown in Fig. 8. The solid line is the prediction of VDM with ρ, ω and φ.

5. The e<sup>+</sup>e<sup>-</sup> → φπ<sup>0</sup> → K<sup>+</sup>K<sup>-</sup>π<sup>0</sup> reaction

The events of this process have been identified by the procedure described above. The only difference is the selected forks have been assumed to be kaons. The peaks in two kaon ef-

fective mass and in missing momentum distribution were seeking for. At the energy 2E = 1.348 GeV the upper limit on the cross-section have been found σ<sub>φπ<sup>0</sup></sub> < 0.5 nb (90 % C. L.).

6. The e<sup>+</sup>e<sup>-</sup> → π<sup>+</sup>π<sup>-</sup>π<sup>+</sup>π<sup>-</sup> and e<sup>+</sup>e<sup>-</sup> → π<sup>+</sup>π<sup>-</sup>π<sup>+</sup>π<sup>-</sup> reactions

Among the 180000 pictures 507 events with three and more prongs were selected. For identification of multiple pion production events the following selection criteria were imposed:

- the events with the point of creation displaced more, than 15 mm from the beam axis are rejected (the resolution on this parameter is equal to 0.3 mm);
- the total charge is equal to ± 1 for three prong events and zero for four prongs;
- the total energy of recorded particles (all of them assumed to be pions) doesn't exceed the total beams energy with the accuracy of the detector resolution.

For selected events the missing mass have been computed. In Fig. 9a,b the distributions of three and four prong events versus missing mass are shown. Left from the boundaries pointed by arrows the events assumed to be candidates for four pions events. Right from the arrows the candidates for five pions events are situated. (the cross-section more than five pions production is negligible in this region). The numbers of events with four (N<sub>4π</sub>) and five (N<sub>5π</sub>) pions are listed in Table 5.

Table 5

2E, GeV	L, nb <sup>-1</sup>	N <sub>4π</sub>	N <sub>5π</sub>	σ <sub>4π</sub> , nb	σ <sub>5π</sub> , nb
1.088	5.4	5	0	2.4+-1.4	-
1.202	24.8	64	1	8.6+-1.2	0.3+0.4-0.3
1.270	23.3	115	3	18.3+-2.3	0.6+-0.5
1.348	25.9	214	7	26.8+-2.2	1.2+-0.7
1.348	36.6	293	9	26.3+-1.9	1.0+-0.5 (including [53])

The computation of efficiency for process of four charged pions production have been performed by the Monte-Carlo method assuming the creation of one intermediate  $\rho^0$ -meson in accordance with [31]. In Fig. 10 the effective mass spectrum for two pions of opposite charges (A), for two pions of the same charge (B) and for three pions are shown. The solid line represents the theoretical prediction. The choosed model fits the experimental data quite good. The efficiency for four pions events within the detector solid angle is equal to 18%, and is 13% for three pions events. The calculation of efficiency for five pions production have been carried out by the LIPS model and was found to be 18%. In calculations the probabilities of track loosing in the spark chamber ( $\sim 10\%$ ), the pion nuclear absorption (2%) and the pion decay in flight ( $\sim 2\%$ ) have been taken into account.

The radiative corrections have been computed in accordance with [32] and have been found to be  $+(3+5)\%$ .

The integrated luminosity, determined by collinear events and experimental cross-sections of four and five pions productions are listed in Table 5.

The systematical error in cross-section of four pions production aroused from the error in the integrated luminosity (3%), error in efficiency computation (5%), uncertainty in radiative corrections (1%) and doesn't exceed 7%. For the process of five pion production the systematical error estimated to be 20%.

In Fig. 11 and Fig. 12 the experimental data on cross-section of four and of five charged pions production in the energy region  $1.0 \leq 2E \leq 2.2$  GeV are shown, correspondingly.

#### 7. The measurement of the neutral kaon mass

In the experiment the neutral kaons have had been produced through the reaction  $e^+e^- \rightarrow K^S K^L$  in the  $\phi$  resonance peak and have been detected by the  $K^S \rightarrow \pi^+\pi^-$  decay. The energy of the initial particles in the storage ring have been measured

by the resonance depolarization method [42,43] and kept constant through all the experiment within the accuracy of 15 keV ( $\Delta E/E = 3 \cdot 10^{-5}$ ). The system of the beam energy stabilization have been described in [44].

There are two substantial features which differ this experiment from previously done [45+48]: 1. the nearness of the kaon mass  $M$  and the beam energy  $E$  and 2. the precise beam energy measurement.

The neutral kaon mass has been determined from the expression

$$M = \sqrt{E^2 - (\vec{p}_+ + \vec{p}_-)^2} = \sqrt{E^2 - p_+^2 - p_-^2 - 2p_+ p_- \cos \psi}$$

where  $p_+$ ,  $p_-$  - the measured momentum of charged pions,  $\psi$  - the angle between pion tracks.

The neutral kaons are produced with low momentum  $P_K = |\vec{p}_+ + \vec{p}_-|$  which is about 5 times less than beam energy, hence the kaon mass

$$M \approx E \left(1 - \frac{P_K^2}{2E^2}\right) = E - \frac{P_K^2}{2E}$$

accuracy is determined by the uncertainty in the beam energy and slightly depends on the pions momentum measurement precision. Moreover, the precise measurement of the beam energy enables to calibrate the detector by the total energy measurement of the two charged pions from the neutral kaons decays or the energy of electron-positron pairs.

The integrated luminosity of the experiment is equal about  $10 \text{ nb}^{-1}$ . The magnetic field was 15 kGs. The detection efficiency of the kaon decays into two pions was approximately 25%. To suppress a background only events with particles momentum in frames  $130+300 \text{ MeV}/c$  were selected. The events with more than three standard deviations of measured points from reconstructed trajectory were rejected. In Fig. 13 the distribution of  $\sim 1200$  selected events versus total energy of two particles (both of them were assumed to be pions) is shown. The peak of neutral kaon decays into two pions is seen as well as low level background connected mainly with pions from

the  $e^+e^- \rightarrow \pi^+\pi^-\pi^0$  reaction.

Comparison of the measured total energy of two pions, as well as average momentum of  $e^+e^-$  pairs, with the beam energy allows to improve the absolute accuracy of the detector in momentum measurements to about 0.1% level.

The mass distribution for events within arrows on Fig. 13 is shown in Fig. 14. The neutral kaon mass has been calculated from the peak events with corrections on detector calibration (-20 keV), emission of  $\gamma$ 's by the initial particles (-74 keV) and found to be

$$M_{K^0} = 497.645 \pm 0.079 \text{ MeV.}$$

The error includes pure statistical (65 keV) and errors due to calibration (26 keV), uncertainty in the detector resolution (30 keV), radiative correction (7 keV) and the beam energy measurement (15 keV).

The experimental data on neutral kaon mass are shown in Fig. 15. The solid lines show direct measurements of the kaon mass and dashed lines show the kaon mass, obtained from the charged and neutral kaon mass difference. The value of the mass difference following from this experiment and world average is equal ( $M_{K^+} = 493.667 \pm 0.015 \text{ MeV}$  [54])

$$M_{K^+} - M_{K^0} = -3.978 \pm 0.080 \text{ MeV.}$$

### 8. Conclusion

The experiments with CMD are in progress. Now a few times greater statistic is under treatment. We hope to improve our results in cross-sections of neutral kaon production as well as cross-sections of multiple pion production. We continue also the neutral kaon mass measurement. The  $100 \text{ nb}^{-1}$  integrated luminosity has been obtained with the precise beam energy determination.

### References

1. G.M.Tumaikin, Proceedings of the tenth international conference on high energy accelerators, Serpukhov, v. 1 (1977) 443.
2. L.M.Barkov et al., NIM 204 (1983) 379.
3. E.A.Kuraev, S.I.Bidelman, Preprint INP 78-82, Novosibirsk (1978).
4. J.E.Augustin et al., Lett. at Nuovo Cimento 2 (1969) 214.
5. D.Benaksas et al., Phys. Lett. 39B (1972) 289.
6. A.Quenzer et al., Phys. Lett. 76B (1978) 512.
7. M.Bernardini et al., Phys. Lett. 46B (1973) 261.
8. D.Bollini et al., Lett. at Nuovo Cimento 14 (1975) 418.
9. A.D.Bukin et al., Phys. Lett. 73B (1978) 226.
10. I.A.Koop et al., Preprint NPI 79-67, Novosibirsk (1979).
11. L.M.Barkov et al., Preprint NPI 79-117, Novosibirsk (1979).
12. I.B.Vasserman et al., Preprint NPI 80-169, Novosibirsk (1980).
13. L.M.Kurdadze et al., Preprint NPI 82-97, Novosibirsk (1982).
14. G.Goundaries, J.Sakurai, Phys. Rev. Lett. 21 (1968) 244.
15. N.M.Budnev et al., Phys. Lett. 64B (1976) 309.
16. V.Barger et al., Phys. Lett. 60B (1975) 89.
17. F.J.Farley, E.Picasso, CERN-EP/79-20 (March 1979).
18. S.Drell, SLAC-PUB-2222, T/E (October 1978).
19. G.Adilov et al., Phys. Lett. 51B (1974) 402.
20. C.Bebek et al., Phys. Rev. 13D (1976) 25.
21. S.F.Bregnev et al., Nucl. Phys. 26 (1977) 547.
22. E.Dally et al., Phys. Rev. Lett. 39 (1977) 1176.
23. V.S.Barashenkov et al., Interaction of high energy particles and atomic nuclei with nuclei, Moskau, 1972.



24. L.M.Barkov et al., Preprint NPI 82-122, Novosibirsk, 1982.
25. B.Esposito et al., Phys. Lett. 67B (1977) 239.  
B.Esposito et al., Lett. Nuovo Cimento 28 (1980) 3377.
26. B.Delcourt et al., Phys. Lett. 99B (1981) 257.
27. P.M.Ivanov et al., Phys. Lett. 107B (1981) 297.
28. F.Mane et al., Phys. Lett. 99B (1981) 261.
29. P.M.Ivanov et al., Preprint NPI 82-50, Novosibirsk, 1982.
30. G.Grosdidier et al., LAL report, 80-35.
31. S.I.Eidelman. Pisma v JETP 26 (1977) 563.
32. J.D.Jacson and D.L.Scharre. NIM 128 (1975) 13.
33. G.Cosme et al., Phys. Lett. 63B (1976) 349.
34. G.Cosme et al., Nucl. Phys. 152B (1979) 215.
35. A.Cordieri et al., Phys. Lett. 81B (1979) 389.
36. A.Cordieri et al., Phys. Lett. 106B (1979) 155.
37. V.A.Sidorov et al., International symposium on lepton and photon interaction at high energies, Batavia, USA (1979).
38. B.Esposito et al., Lett. Nuovo Cimento 25 (1979) 5.
39. B.Esposito et al., Lett. Nuovo Cimento 28 (1980) 195.
40. C.Bacci et al., Phys. Lett. 95B (1980) 139.
41. A.Cordier et al., LAL 81/20 June 1981.
42. A.D.Bukin et al., Pros. 5th. Int. Symp. on high energy and elementary particle physics, Warsaw (1975) 138.
43. Ya.S.Derbenev et al., Preprint NPI, 76-64, Novosibirsk (1976).
44. B.A.Baklakov et al., Proceedings of the 7 Allunion conference on high energy accelerators, Dubna, v. 1 (1980) 338.
45. J.H.Christenson et al., Phys. Lett. 13 (1964) 138.
46. J.K.Kim et al., Phys. Rev. 140B (1965) 1334.
47. C.Baltay et al., Phys. Rev. 142B (1966) 932.

48. V.L.Fitch et al. Phys. Rev. 164B (1967) 1711.
49. A.H.Rosenfeld et al., Phys. Rev. Lett. 2 (1959) 110.
50. F.S.Crowford et al., Phys. Rev. Lett. 2 (1959) 112.
51. R.A.Burnstein et al., Phys. Rev. 138B (1965) 895.
52. D.G.Hill et al., Phys. Rev. 168 (1968) 1534.
53. L.M.Barkov et al., Preprint NPI 82-124, Novosibirsk (1982).
54. 'Review of Particle properties', Phys. Lett. 111B, April 1982.

Figure captions

Fig. 1. The horizontal schematic cross sections of the detector. 1-high voltage feeding, 2-joke, 3-nitrogen shell, 4-magnetic lens of the storage ring, 5-compensating solenoid, 6-spark chamber, 7 - main solenoid, 8-outer mwpc, 9-inner mwpc 10-optic lens, 11-mirror.

Fig. 2. The collinear events distribution on average momentum at  $2E = 0.430, 0.700$  and  $0.820$  GeV.

Fig. 3. The squared form factor of the charged pion versus the total energy  $2E$ .

Fig. 4. The experimental data on the  $\langle v_{\pi} \rangle^2$  value.

Fig. 5. The collinear events distribution on average momentum at  $2E = 1.088, 1.202, 1.270, 1.348$  GeV.

Fig. 6. The squared form factor of the charged kaon versus the total energy  $2E$ .

Fig. 7. The effective mass distribution for: A-events after selection B-events not selected.

Fig. 8. The squared form factor of the neutral kaon versus the total energy  $2E$ .

Fig. 9. The missing <sup>mass</sup> distribution for: A-three prong events, B-four prong events.

Fig. 10. The effective mass for A-pairs of pions with the different charges, B-pairs of pions with the same charges, C- three pions. The solid line - calculation.

Fig. 11. The  $e^+e^- \rightarrow \pi^+\pi^-\pi^+\pi^-$  cross section versus the total energy.

Fig. 12. The  $e^+e^- \rightarrow \pi^+\pi^-\pi^+\pi^0$  cross section versus the total energy.

Fig. 13. The total energy distribution for two pions.

Fig. 14. The mass distribution for two pions.

Fig. 15. The experimental data on the neutral kaon mass.

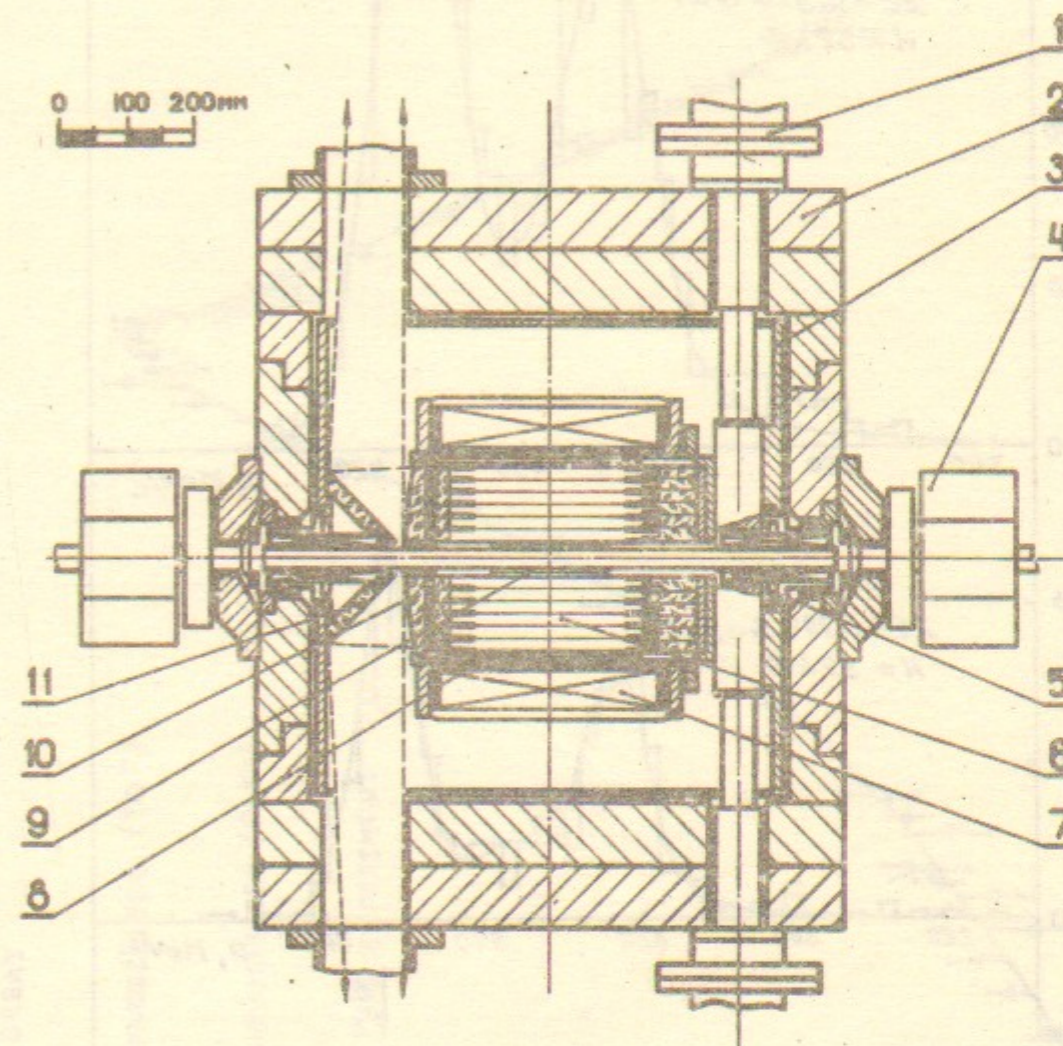


Fig. 1

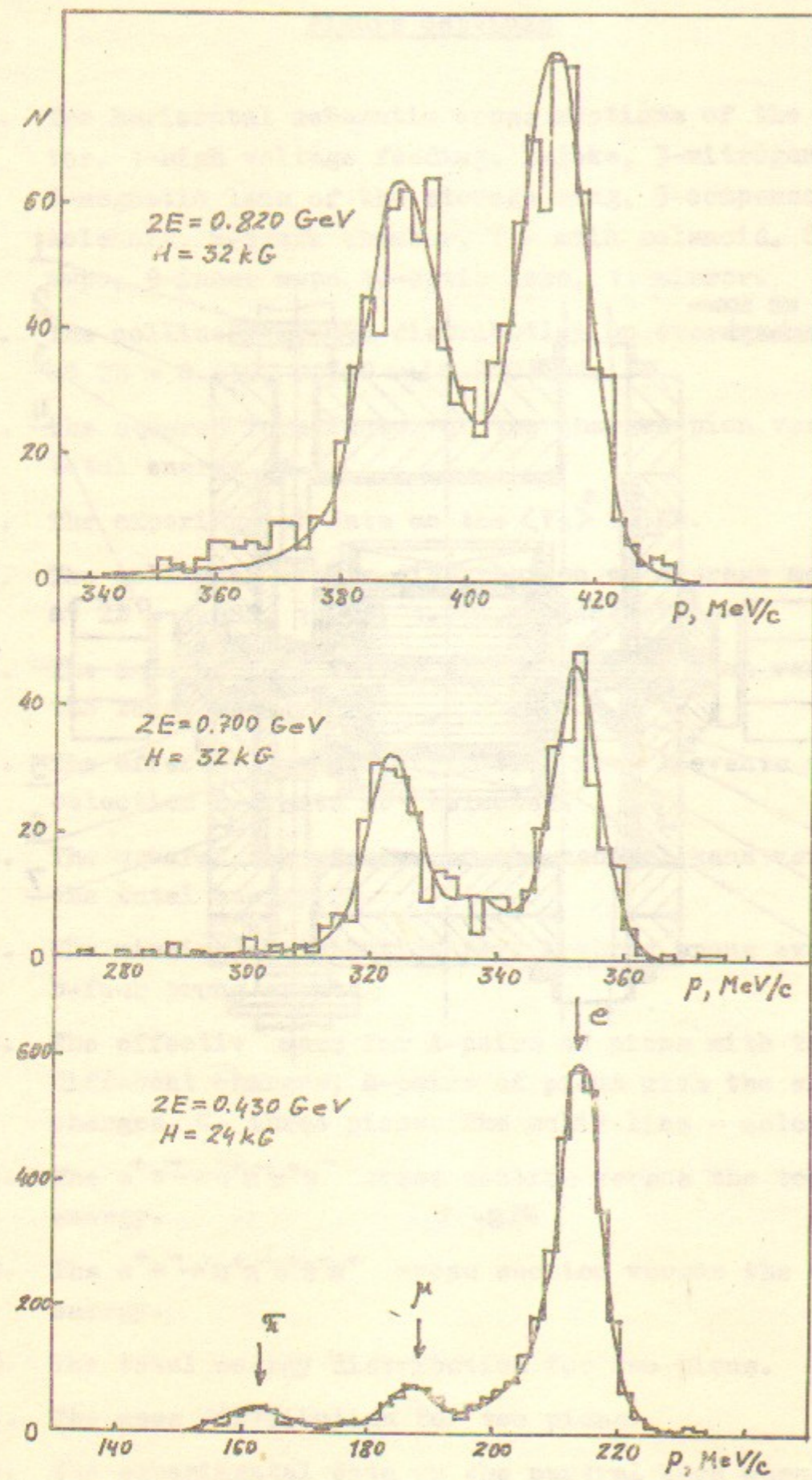


Fig. 2

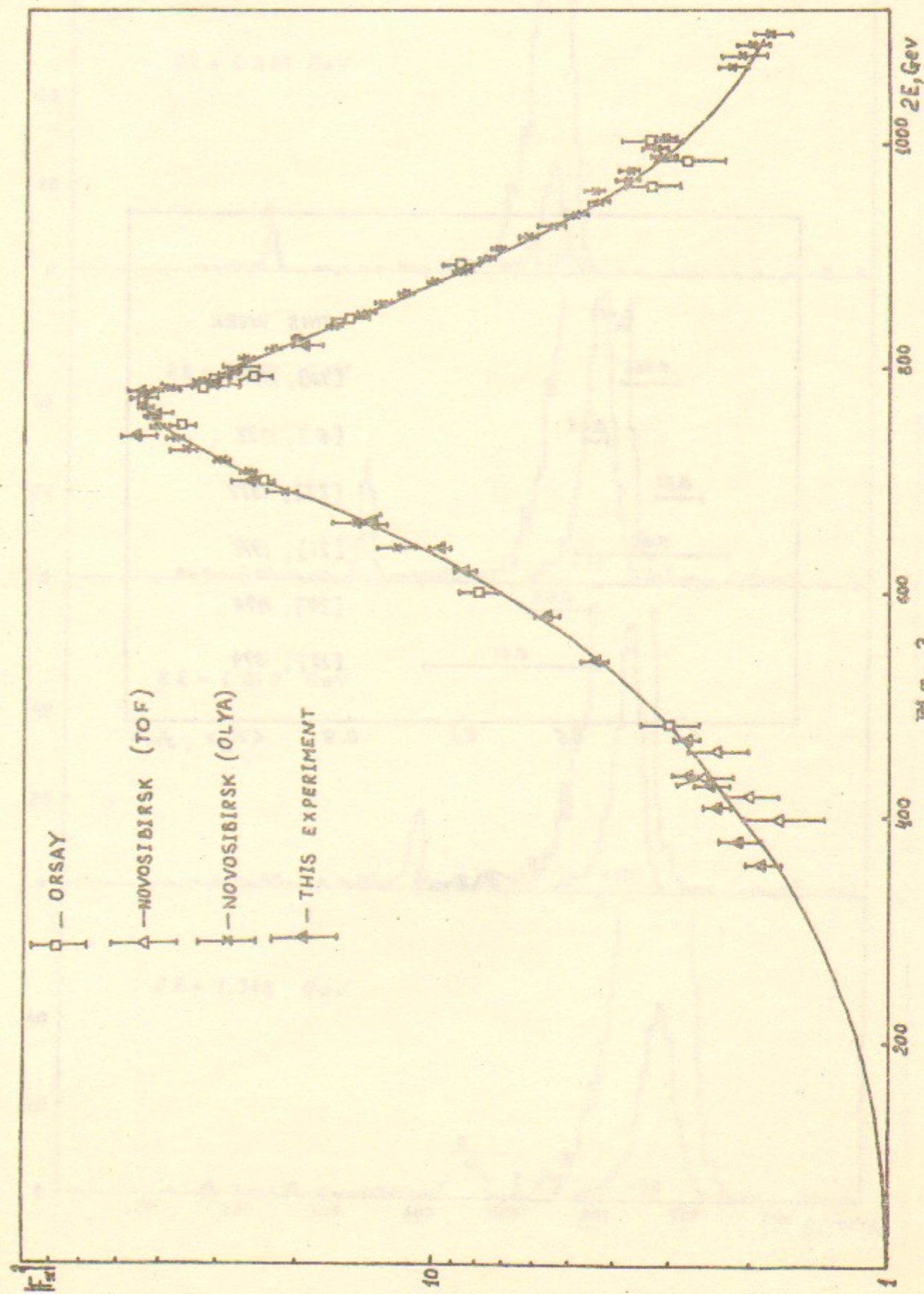


FIG. 3

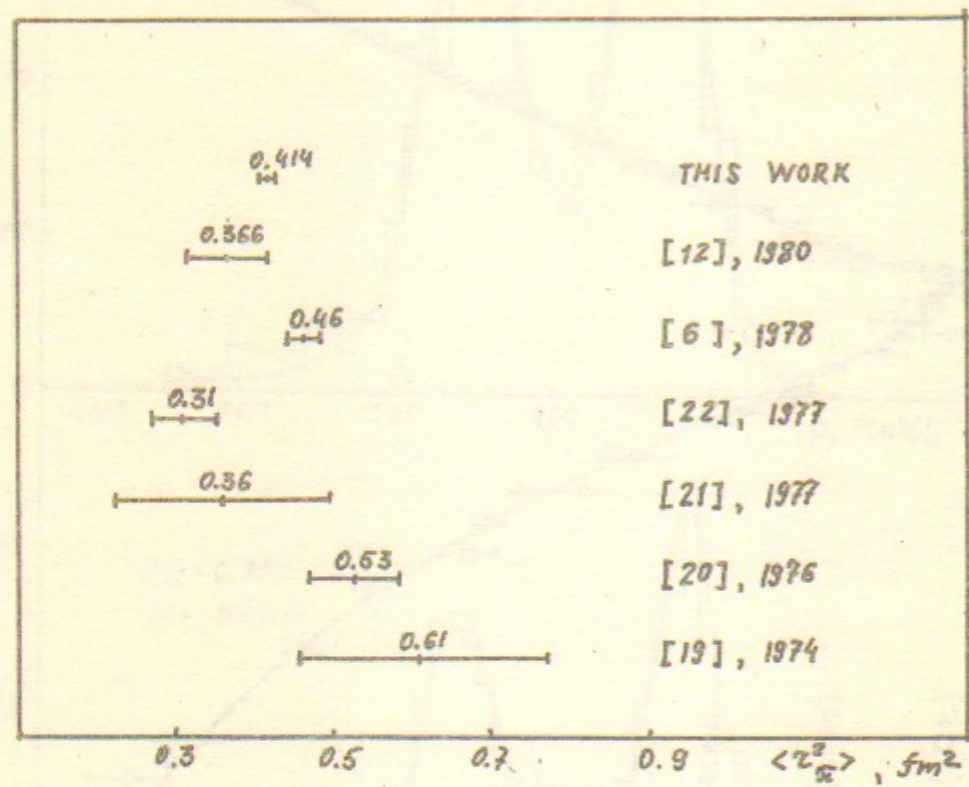


Fig. 4

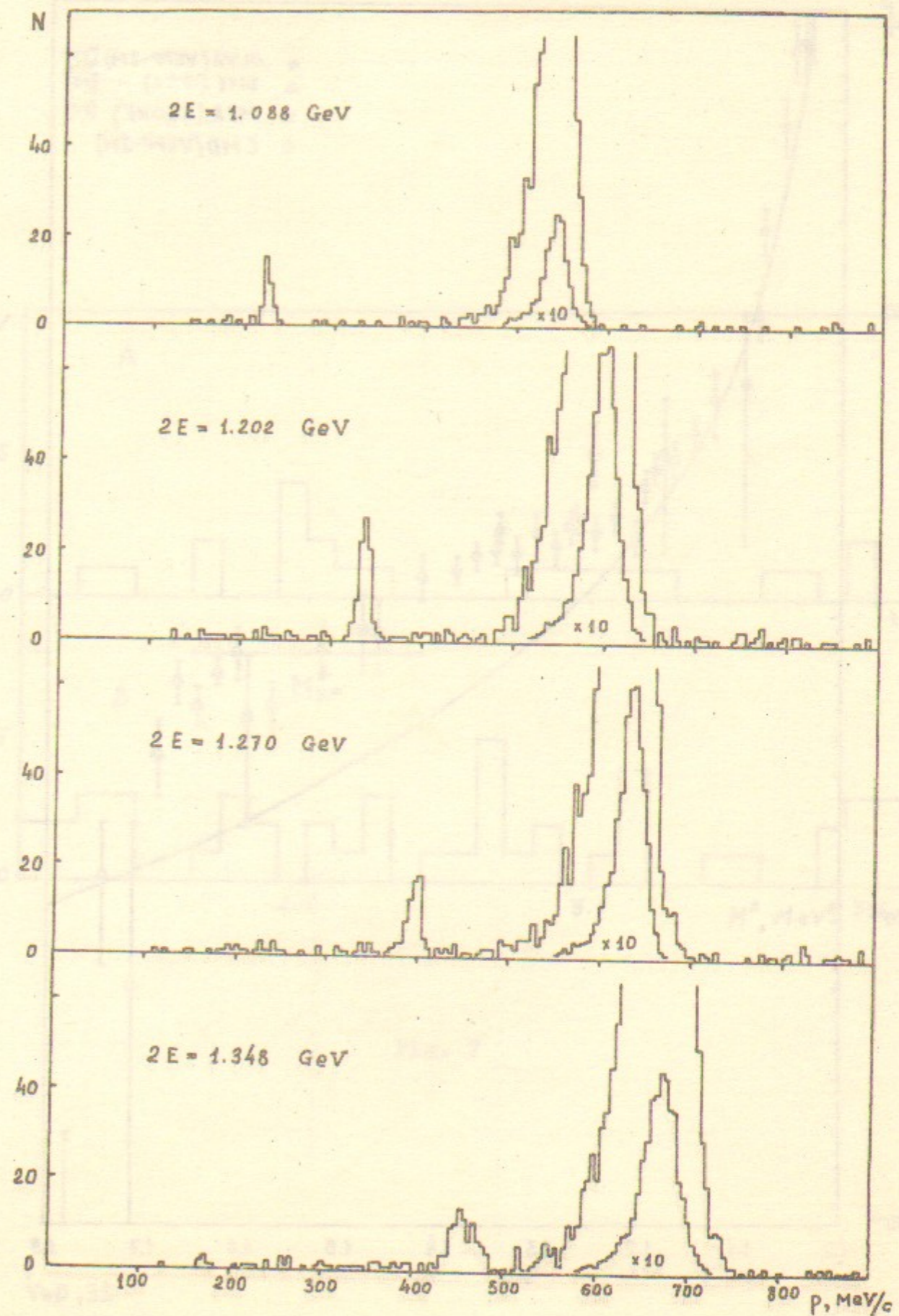


Fig. 5

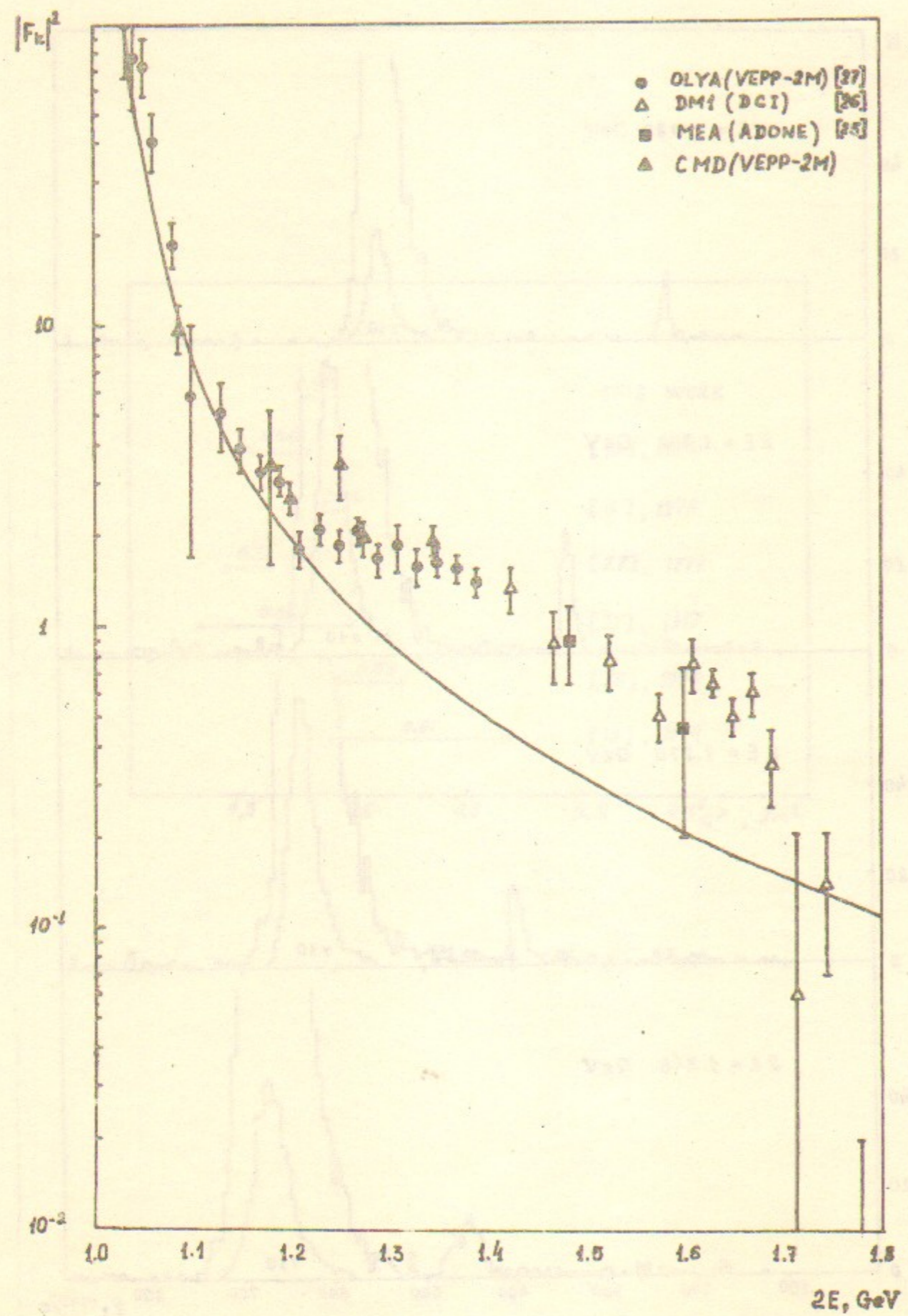


Fig. 6

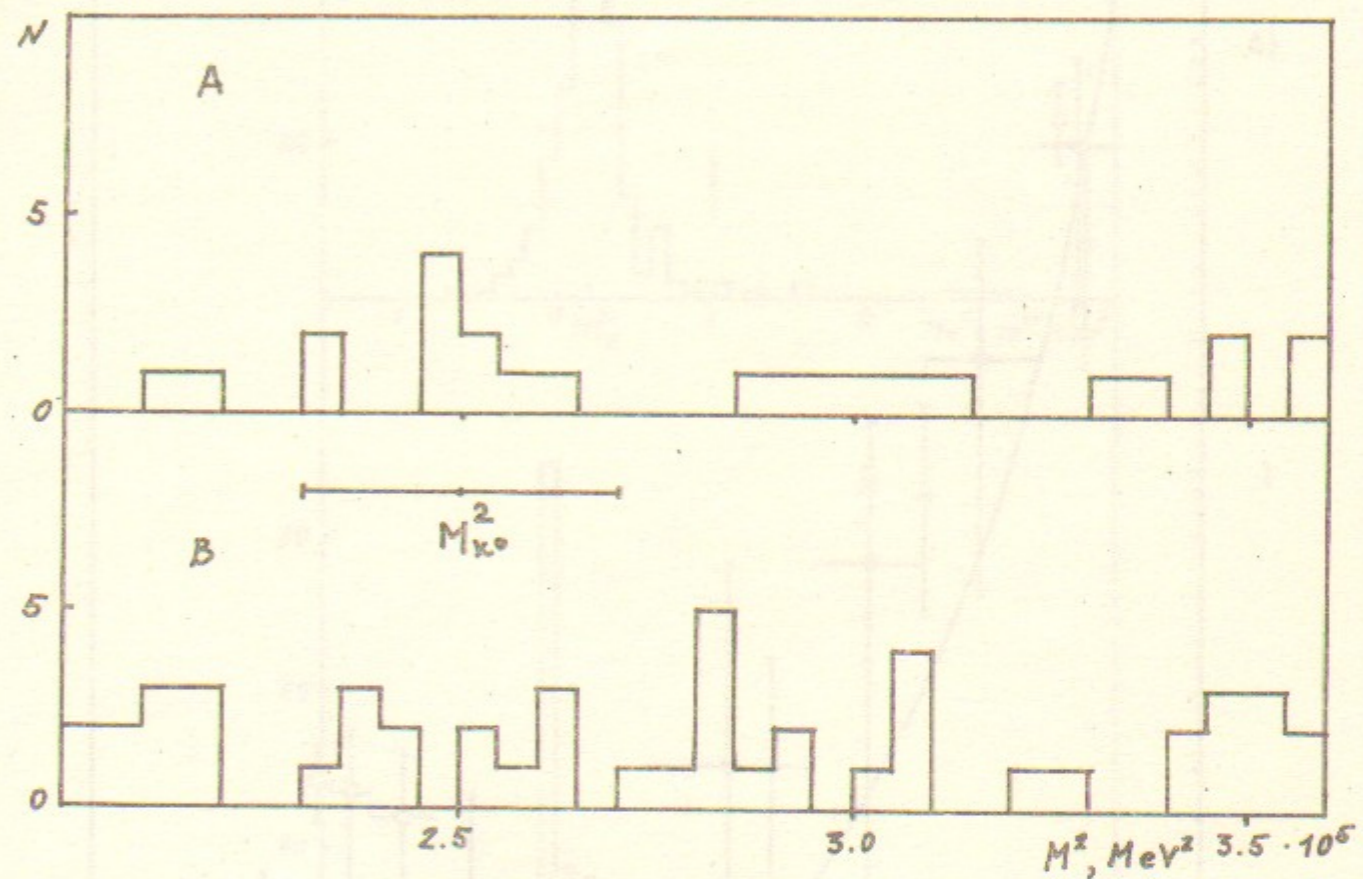


Fig. 7

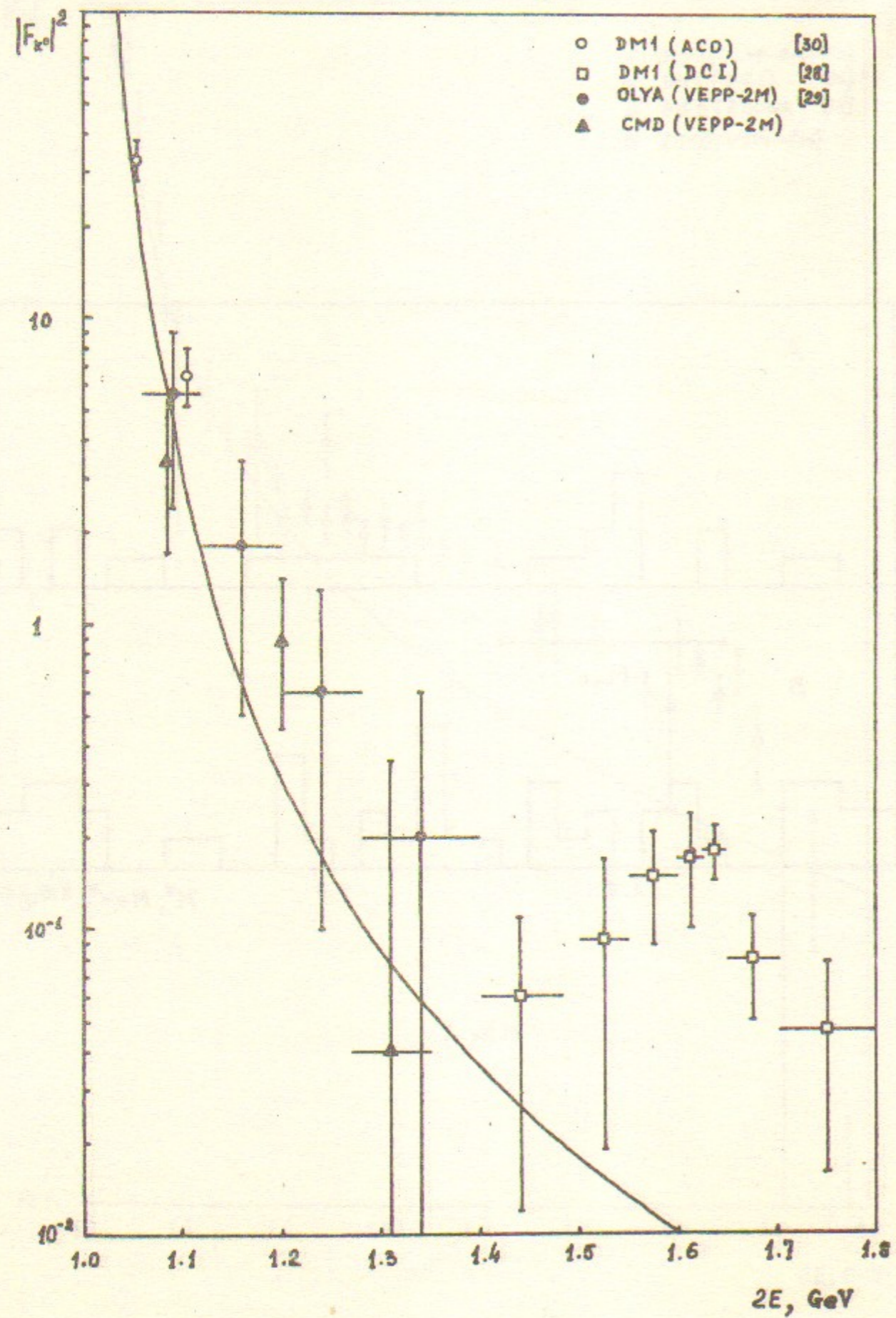


Fig. 8.

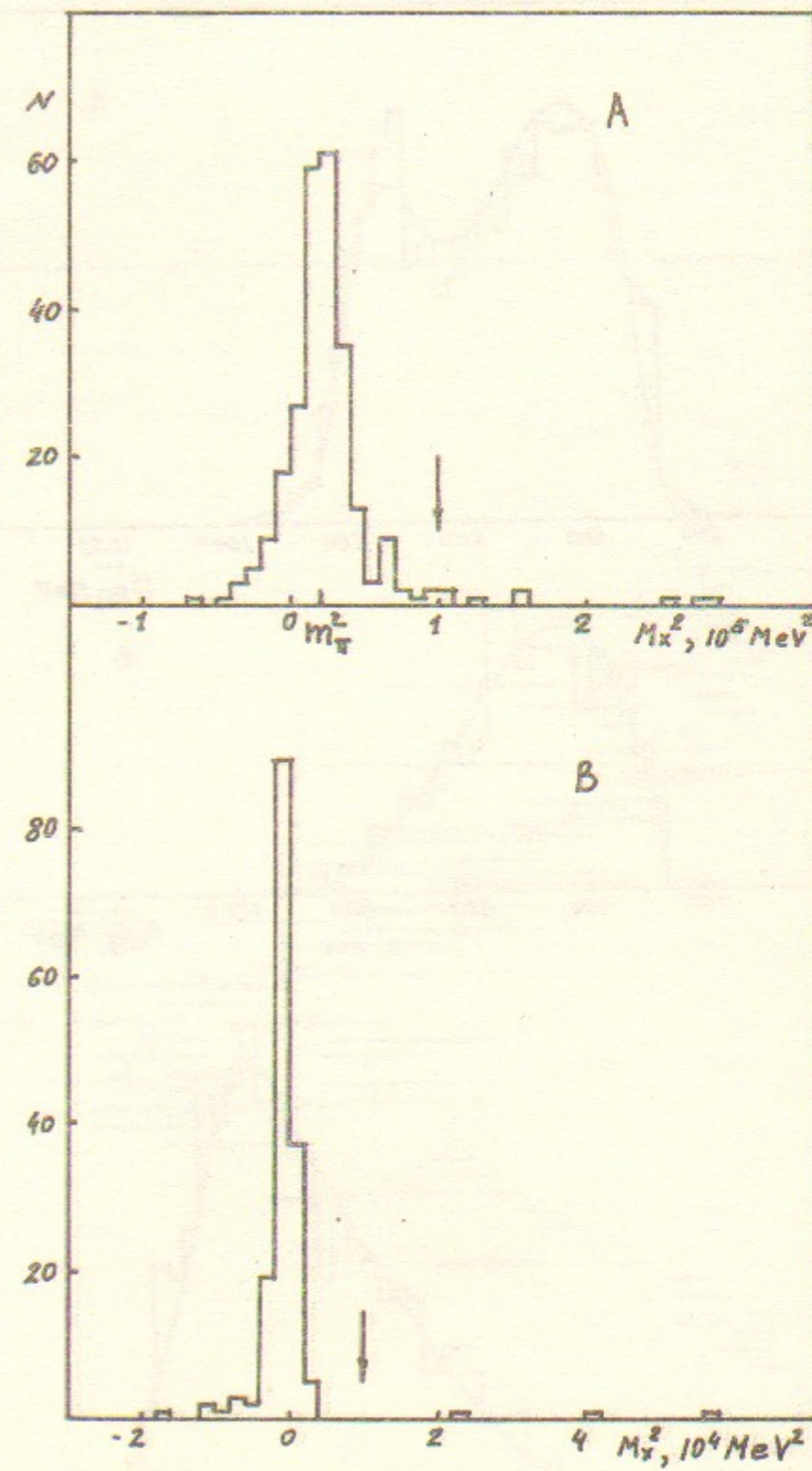


Fig. 9

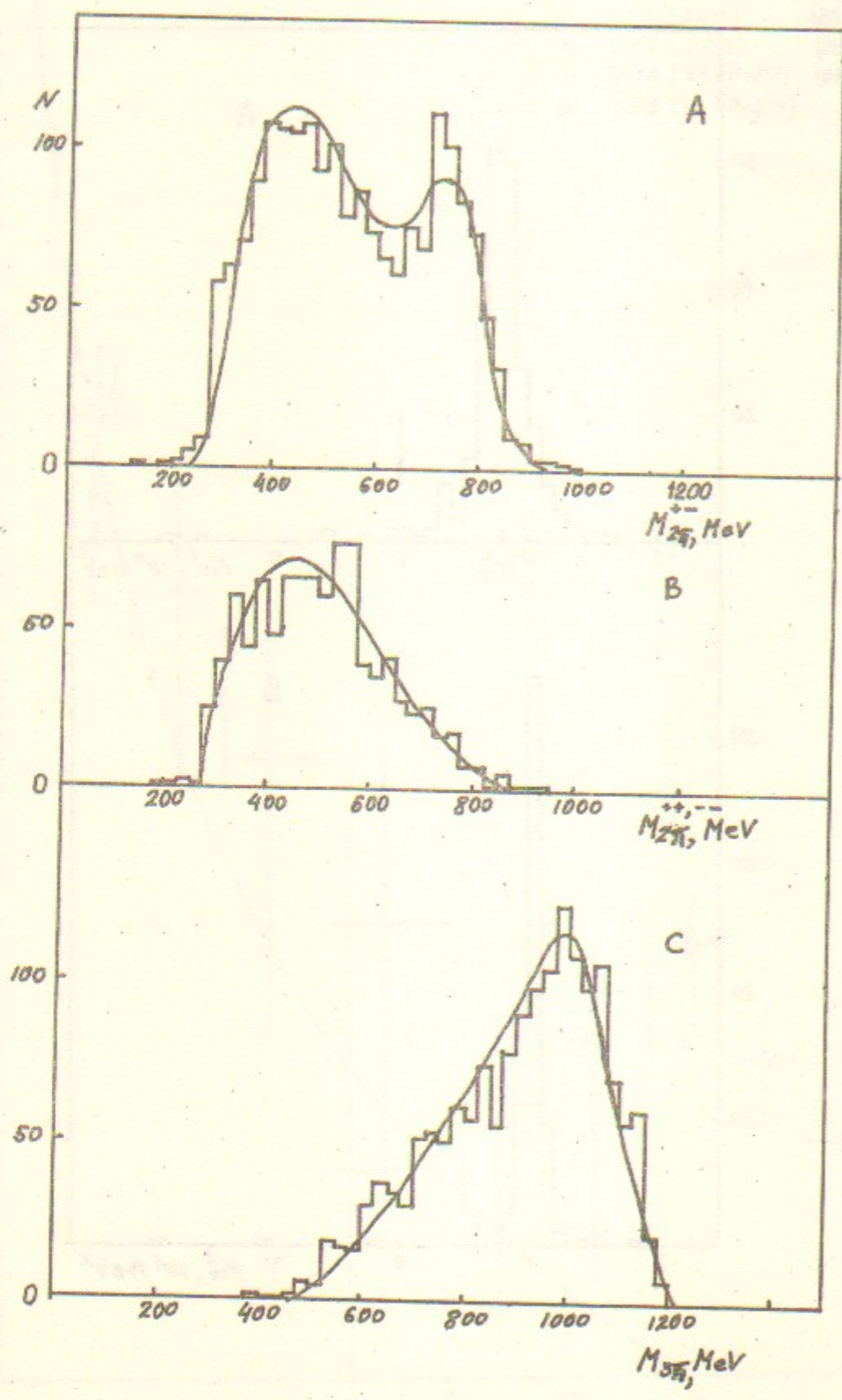


Fig. 10

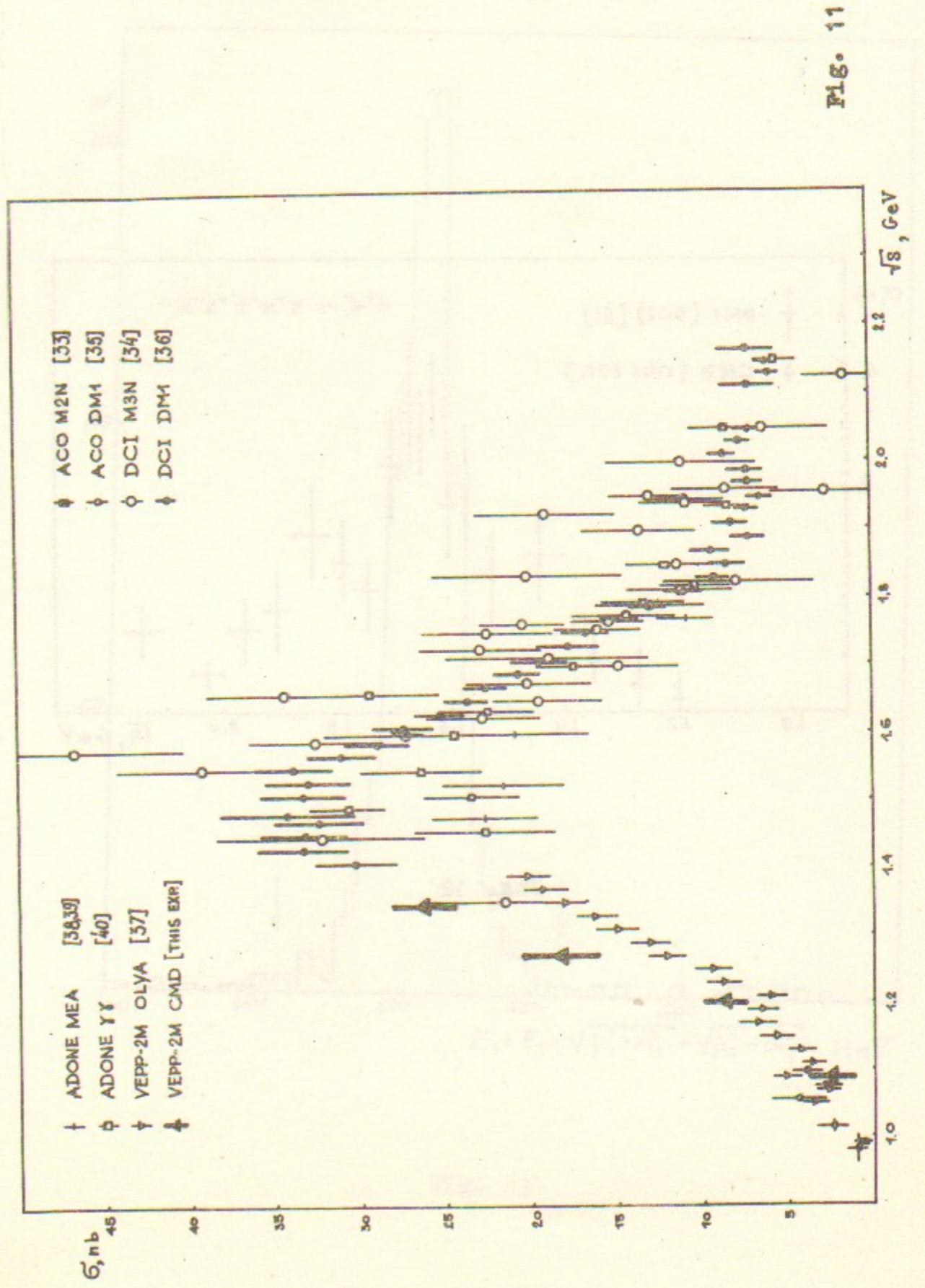


Fig. 11

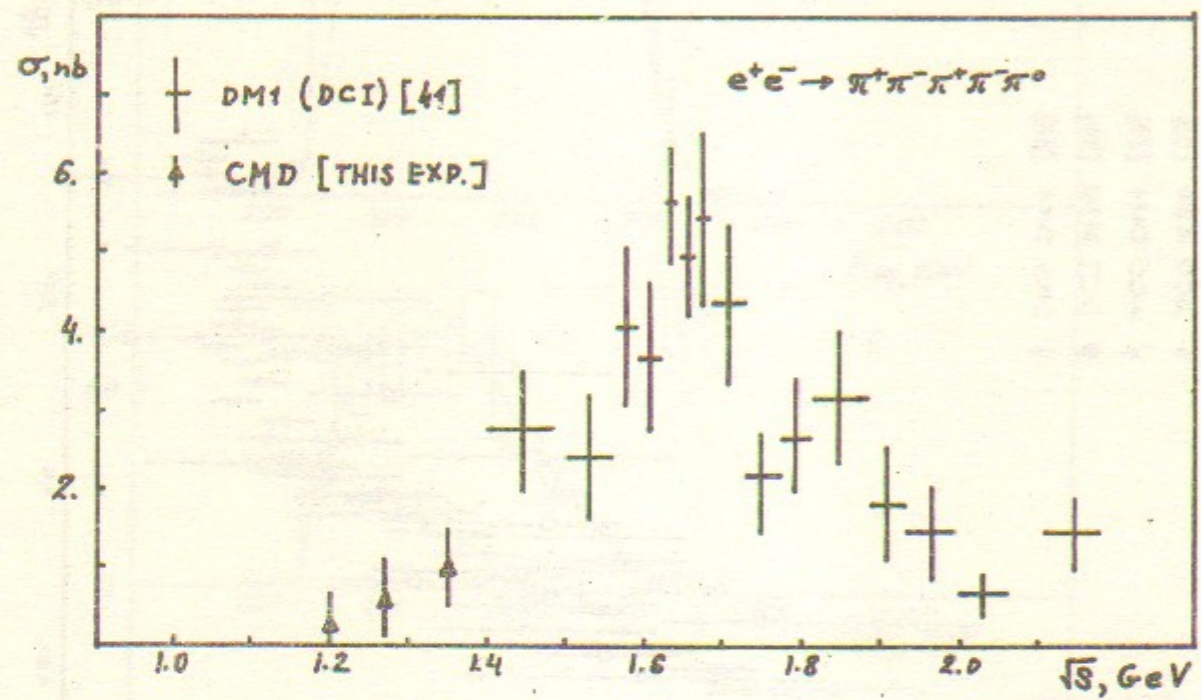


Fig. 12

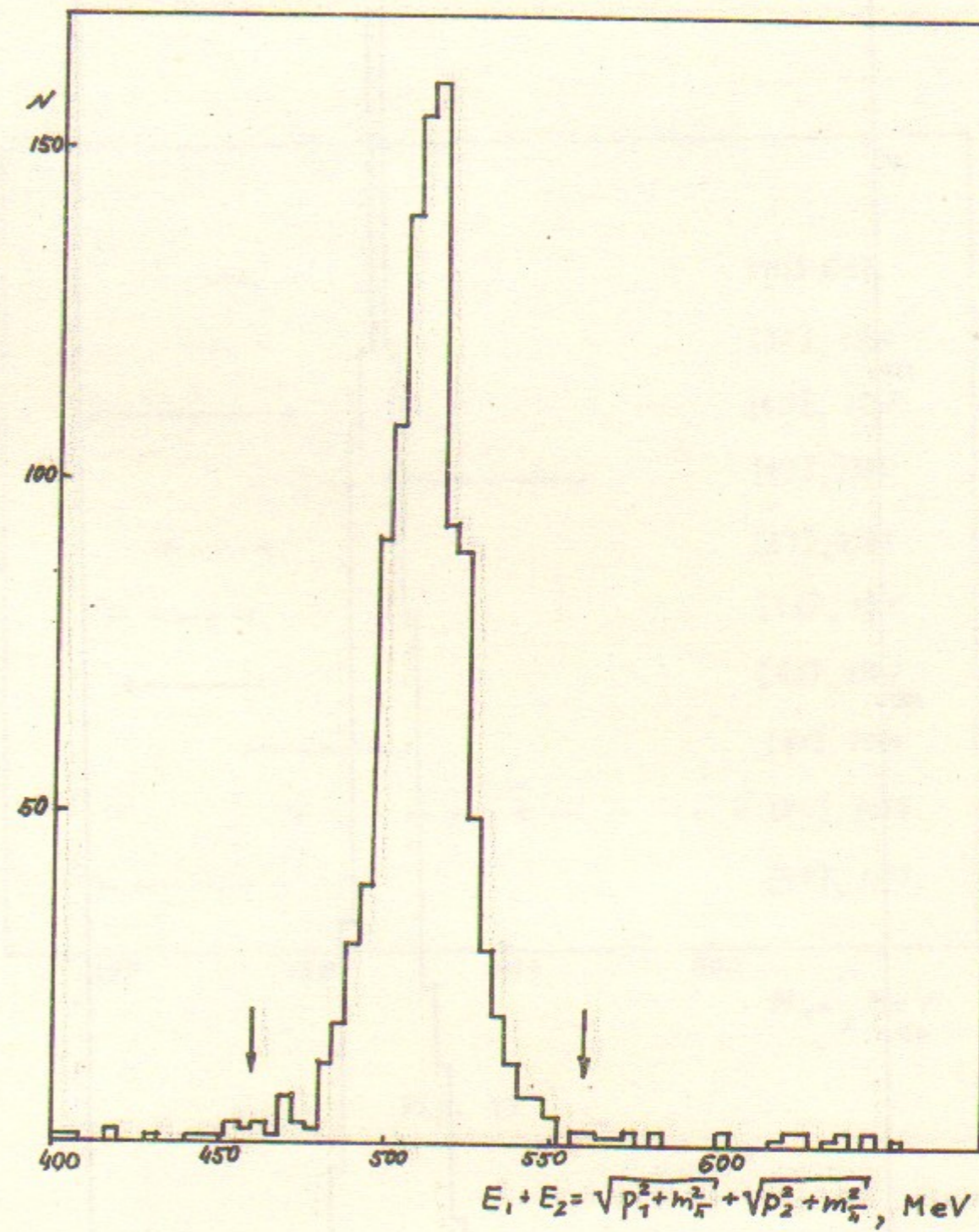


Fig. 13



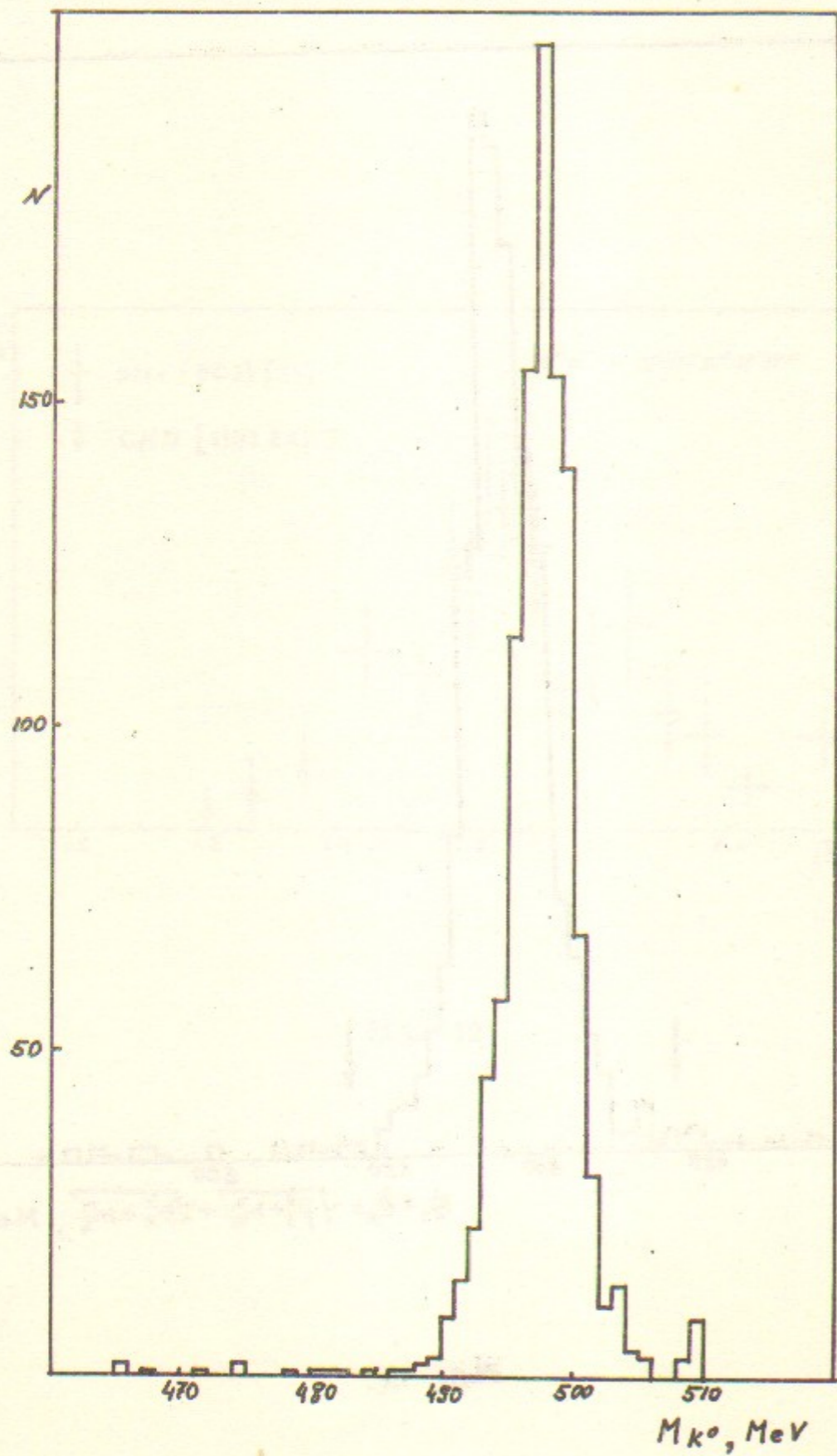


Fig. 14

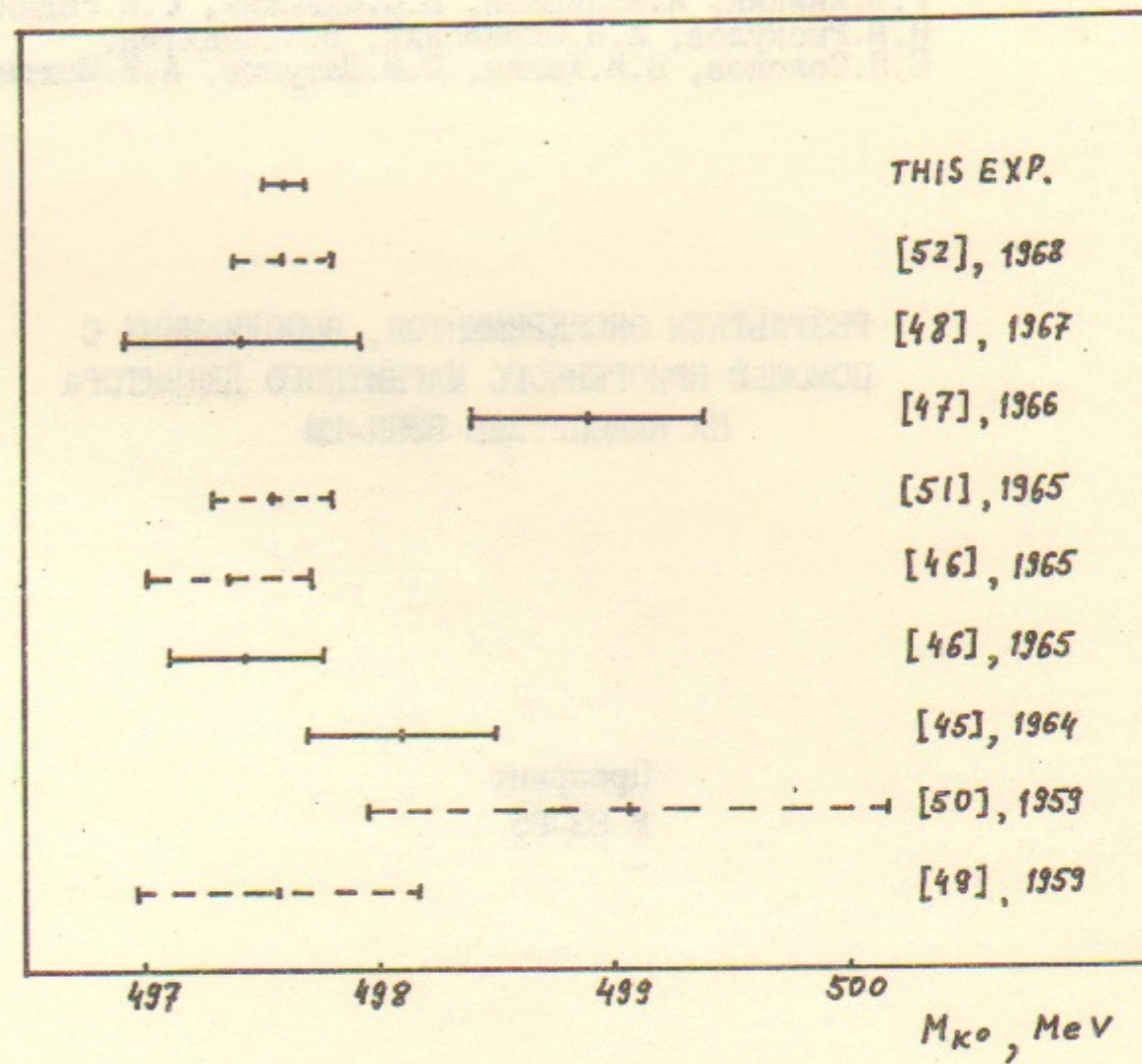


Fig. 15

Г.В.Аникин, Л.М.Барков, В.С.Охапкин, С.И.Редин,  
Н.М.Рыскулов, А.Н.Скринский, В.П.Смахтин,  
Е.П.Солодов, Б.И.Хазин, Ю.М.Шатунов, А.И.Шехтман

РЕЗУЛЬТАТЫ ЭКСПЕРИМЕНТОВ, ВЫПОЛНЕННЫХ С  
ПОМОЩЬЮ КРИОГЕННОГО МАГНИТНОГО ДЕТЕКТОРА  
НА НАКОПИТЕЛЕ ВЭП-2М

Препринт  
№ 83-85.

Работа поступила - 18 июля 1983 г.

---

Ответственный за выпуск - С.Г.Попов

Подписано к печати 22.07-1983 г. МН 03264

Формат бумаги 60x90 1/16 Усл.1,5 печ.л., 1,2 учетно-изд.л.

Тираж 290 экз. Бесплатно. Заказ № 85.

---

Ротапринт ИЯФ СО АН СССР, г.Новосибирск, 90